

# Basement Membrane–Dependent Survival of Retinal Ganglion Cells

Willi Halfter,<sup>1</sup> Michael Willem,<sup>2</sup> and Ulrike Mayer<sup>3</sup>

**PURPOSE.** The present study investigates the role of the inner limiting membrane (ILM) in the survival of ganglion cells (GCs) in embryonic chick and mouse retina.

**METHODS.** In chick embryos, the ILM was enzymatically removed at embryonic day (E)5 and E7 in ovo, and GCs were counted over the following 7 days of incubation. In mice, the ILM ruptured early in development due to a targeted mutation of laminin- $\gamma$ 1. The number of surviving GCs in late embryonic homozygous mutant mice was compared to GC counts in heterozygous and nonmutant siblings. The survival of GCs was also assayed in vitro, using the ILM as a substrate.

**RESULTS.** When the ILM was removed in E5 chick embryos, almost all GCs underwent apoptosis by E10. GC apoptosis was prevented by reconstituting the ILM shortly after its disruption. Apoptosis of retinal GCs also occurred in mouse embryos with a fragmented ILM. ILM disruption in both chick and mice not only affected GC survival but also led to the retraction of the end-feet processes of radial cells from the GC layer. In vitro, GCs thrived better on substrates of radial cell end feet than on plain ILM, indicating that the contact with the end feet is more important than the presence of the ILM for GC survival.

**CONCLUSIONS.** The radial cell end feet are the natural substrate for GCs and are essential for their survival. The importance of the ILM lies in its function to anchor the radial end feet to the vitreal surface of the retina. (*Invest Ophthalmol Vis Sci.* 2005; 46:1000–1009) DOI:10.1167/iovs.04-1185

Basement membranes (BMs) are 50-nm-thick extracellular matrix sheets that comprise members of the laminin family, collagen IV, collagen XVIII, nidogen, agrin, and perlecan.<sup>1,2</sup> Whereas the laminin family members have a function in cell adhesion,<sup>3</sup> the collagens provide the scaffold that is critical for the mechanical stability of BMs.<sup>4,5</sup> Data suggest that nidogen with its binding sites for collagen IV and laminin is the linker between the laminins and the collagen IV network.<sup>6,7</sup> Although targeted deletions of perlecan, agrin, and collagen XVIII have been described, their functions in BM assembly and stability are unclear.<sup>8–11</sup>

From the <sup>1</sup>Department of Neurobiology, University of Pittsburgh, Pittsburgh, Pennsylvania; the <sup>2</sup>Department of Biochemistry, Adolph-Butenandt Institute, Laboratory for Alzheimer's and Parkinson's Disease Research, Ludwig-Maximilians University, Munich, Germany; and the <sup>3</sup>Wellcome Trust Centre for Cell-Matrix Research, University of Manchester, Manchester, United Kingdom.

Supported by Grants IBN-0240774 from the National Science Foundation (WH), MA 1707/1-1 and 1-2 from the Deutsche Forschungsgemeinschaft (UM); and 060549 from the Wellcome Trust (UM).

Submitted for publication October 6, 2004; revised November 15, 2004; accepted November 21, 2004.

Disclosure: **W. Halfter**, None; **M. Willem**, None; **U. Mayer**, None

The publication costs of this article were defrayed in part by page charge payment. This article must therefore be marked "advertisement" in accordance with 18 U.S.C. §1734 solely to indicate this fact.

Corresponding author: Willi Halfter, Department of Neurobiology, University of Pittsburgh, 1402 E Biological Science Tower, Pittsburgh, PA 15261; whalfter@pitt.edu.

BMs in the central nervous system comprise the numerous vascular BMs in brain, the pial BM, and the retinal BM, also referred to as the inner limiting membrane (ILM). Recent data in chick embryos have shown that the ILM and pial BM are important in the development of the nervous system, as they serve as an attachment site for the end feet of the neuroepithelial and radial glia cells. In addition, the BMs prevent growing axons and migrating neurons from aberrantly exiting into the adjacent connective tissues.<sup>12–14</sup> The abundance of cortical and retinal dysplasias in mice with mutations in BM proteins<sup>9,14</sup> and their receptors<sup>15–17</sup> confirms the importance of BMs in containing axons, neurons, and glia cells within the confines of the CNS.

Our laboratories have studied the ILM of the embryonic chick eye as a model system to determine the function of BMs in the developing CNS. Based on experiments disrupting the ILM in ovo, we established that the ILM is essential for retinal histogenesis and the navigation of optic axons.<sup>12,18</sup> In previous studies, experiments were usually terminated between 2 and 3 days after ILM disruption.

In a new set of experiments, we investigated the long-term effects of ILM removal on retinal development. Unexpectedly, we found that the presence of the ILM is essential in the survival of retinal ganglion cells (GCs). The importance of the ILM in GC survival was confirmed by showing that in mice with a mutation-induced disrupted ILM the number of GCs is also greatly reduced.

## METHODS

### Antibodies

The following monoclonal antibodies (mAbs) were used: 3H11 to laminin-1,<sup>19</sup> 1G12 to nidogen-1,<sup>20</sup> 6C4 to collagen XVIII,<sup>21</sup> 6D2 to agrin,<sup>19</sup> 4H6 to neurofilament,<sup>19</sup> and 6G7 to  $\beta$ -tubulin.<sup>14</sup> The mAb 1D10 to chick CD44 served as a marker for macrophages. Its antigen specificity was established by cDNA cloning (accession code for the cDNA in GeneBank, AF 153205; <http://www.ncbi.nlm.nih.gov/Genbank>; provided in the public domain by the National Center for Biotechnology Information, Bethesda, MD; Zhu S and Halfter W, unpublished data, 1999). The mAbs are available from the Developmental Studies Hybridoma Bank (University of Iowa, Iowa City, IA). The mAb 9H2 to NCAM-180 was used to stain chick and mouse retina ganglion cells in vivo and in vitro. Its antigen specificity was established by Western blot analysis (Halfter W, unpublished data, 1998). mAbs to Brn3a,<sup>22</sup>  $\beta$ -dystroglycan, and Mac3 were obtained from Chemicon (Temecula, CA) and BD Pharmingen (San Diego, CA), and rabbit antisera to mouse laminin-1 and cleaved caspase-3 (ASP175) were purchased from Invitrogen-Gibco (Gaithersburg, MD) and Cell Signaling Technology (Beverly, MA), respectively. mAbs to islet 1 (4D5), vimentin (H5), visinin (7G4), AP-2 (3B5), and  $\beta$ 1 integrin (JG22) were obtained from the Developmental Studies Hybridoma Bank. The nuclear counterstain used (Sytox green) was obtained from Molecular Probes (Eugene, OR).

### Disruption and Regeneration of the Retinal Basement Membrane In Vivo

The ILM in chick was enzymatically removed by injecting 0.5  $\mu$ L of 100 U/mL recombinant collagenase (Sigma-Aldrich, St.

Louis, MO) into eyes of embryonic day (E)5 and E7 chick embryos.<sup>12</sup> Only the right eye of an embryo was injected, whereas the left, contralateral eye served as the control. For ILM regeneration experiments, collagenase was injected as described earlier followed 10 hours later by a second injection of 2  $\mu$ L of a mixture of mouse laminin-1 (Invitrogen-Gibco) and  $\alpha$ 2-macroglobulin (Sigma-Aldrich) at a final concentration of 1 mg/mL each.<sup>18</sup> Macroglobulin serves as an inhibitor for the injected collagenase and does not participate in ILM regeneration. The embryos were killed 24 hours to 7 days after the collagenase injections or the laminin chases, and sections through the eyes were stained with antibodies to laminin-1, nidogen-1, collagen XVIII, and agrin, to determine the presence or absence of the ILM.

### Mutant Mice

The mutation in laminin was generated by deleting the 56-amino-acid nidogen-binding module  $\gamma$ 1III4 in the LAMC1 gene, as previously described.<sup>23</sup> Litter mate mutant and control embryos of E16.5 ( $n = 17$ ) were investigated. Homozygous mutant embryos were differentiated by their red eyes and small body size from the clear-eyed, normal-sized heterozygous and non-mutant littermates. The identity of mutants, heterozygotes, or nonmutant mice was always confirmed by genotyping.<sup>23</sup>

### Histology

Heads and dissected retinas from chick and mouse embryos were fixed in 4% paraformaldehyde and processed as described.<sup>18</sup> Cryostat sections were permeabilized with 0.05% Triton-X-100 and 1% BSA for 10 minutes and incubated with hybridoma supernatants or primary antisera for 1 hour. After three rinses, the sections were incubated with 1:500 Cy3-labeled goat-anti mouse or goat-anti rabbit antibodies (Jackson ImmunoResearch, West Grove, PA) for another hour. The specimens were mounted in 90% glycerol and examined with an epifluorescence or a confocal microscope (Flowview; Olympus, Tokyo, Japan). Up to E8, chick retinal GCs were identified by staining for islet 1<sup>24</sup> and from E8 onward by staining for Brn3a.<sup>22</sup> Islet-1- and Brn3a-positive GCs were counted at 400 $\times$  for a defined length of the retina (400  $\mu$ m) at two positions approximately 300 to 400  $\mu$ m away from the optic disc. Between 3 and 10 embryos were processed at each time point. Apoptosis was quantified by counting the number of activated caspase-3-positive cells per cross section through the retina of the experimental eyes, and macrophage invasion was measured by counting CD44<sup>+</sup> cells in a defined area of 400  $\times$  400  $\mu$ m in retinal wholemounts. Radial cells were stained in total with an antibody to vimentin (clone H5; Developmental Studies Hybridoma Bank), whereas individual radial cells were labeled with DiI.<sup>18</sup>

For mouse embryos, GCs were backlabeled by applying DiI to the optic nerve. The eyes were incubated for 2 days in 4% paraformaldehyde in Ca<sup>2+</sup> and Mg<sup>2+</sup>-free Hanks solution (CMF) at 37°C, the retinas dissected and flatmounted, and the labeled cells counted at 200 $\times$  for a defined area of 150  $\mu$ m<sup>2</sup>. GCs were also counted in 1- $\mu$ m-thin sections of EPON-embedded retinas at 400 $\times$  for a retinal segment of 70  $\mu$ m. The criteria for GC identification in thin sections were location in the GC layer and a pale euchromatic nucleus with prominent nucleolus, clearly distinctive from the heterochromatic nucleus of the undifferentiated neuroepithelial cells.

### Cell Culture

Substrates for cell culture were (1) E8 chick ILM with neuroepithelial end feet, (2) ILM without end feet, and (3) laminin-1 (20  $\mu$ g/mL; Invitrogen-Gibco) on poly-L-lysine. The preparation

ILM with end feet is obtained by a mechanical cleavage of retinal wholemounts and consists of the ILM covered by a monolayer of neuroepithelial end feet.<sup>25</sup> On treatment with 2% Triton-X-100, the end feet are removed, leaving behind the plain ILM.<sup>25</sup> The substrates, outlined by a hydrophobic border (PAPpen; EMS, Washington, PA), had a surface area of approximately 1 cm<sup>2</sup>. GCs from E7 chick embryos were obtained by consecutive cleavage of trypsinized retinal wholemounts.<sup>26</sup> They were cultured on the three different substrates at a density of 2000 cells per culture in 125  $\mu$ L serum-free DMEM for 1 to 7 days. After fixation in 4% paraformaldehyde, GCs were detected by immunostaining with the mAbs 6G7 to tubulin, 9H2 to NCAM-180, 4H6 to neurofilament, and 4D5 to islet 1. Labeled cells were counted for a defined microscopic field and plotted in percentages using the number of surviving neurons on ILM with end feet as a 100% reference.

## RESULTS

### Removal and Regeneration of the ILM in the Embryonic Chick Eye

The ILM in chick embryos was removed by injecting recombinant clostridial collagenase into the vitreous of E3 and E7 eyes ( $n = 261$ ).<sup>12</sup> The collagenase resulted in the digestion of collagen IV and XVIII within an hour, followed by the dissociation of the remaining ILM components within 2 hours. The treated eyes were unable to reassemble the missing ILM during further incubation (Fig. 1a;  $n = 65$ ). The ILM regenerated within 6 hours when the collagenase was followed by a chase injection of mouse laminin-1 ( $n = 105$ ).<sup>18</sup> The regenerated ILM assembled 50  $\mu$ m below the vitreal surface and remained at this position throughout further development (Fig. 1c). The regenerated ILM was ultrastructurally indistinguishable from the control ILM and comprised all components of a normal chick ILM, such as laminin-1, nidogen-1, collagen IV, collagen XVIII, and agrin.<sup>18</sup>

The surface of an E5 chick retina expands fourfold during the following 5 days of incubation, predominantly by adding new cells to its periphery. When eyes of E5 chick embryos were injected with collagenase and the embryos examined at E10 or later, the retinas of the experimental and contralateral control eyes had grown to identical sizes. Further, the central portion of the retinas from the experimental eyes had no ILM, as expected (Fig. 1a). However, the newly developed, peripheral parts of the experimental retinas had no ILM either (Fig. 1b;  $n = 45$ ). Thus, when the ILM was removed at an early stage, the eyes were unable to generate any ILM.

When eyes were injected with collagenase at E5 followed by a laminin-1 chase 10 hours later, an ectopically located ILM reconstituted in central part of the E10 retinas (Fig. 1c), whereas a continuous and normally located ILM formed in the newly generated, peripheral retina (Fig. 1d;  $n = 35$ ). Based on its location, we assume that the peripheral ILM is generated de novo. The transition between the regenerated and normally located ILM was in the range of <100  $\mu$ m (Fig. 1e).

### Retraction of Radial Cells after ILM Removal

Vimentin staining of E10 control retinas revealed a regular array of radially organized cells (Fig. 2a). These cells are neuroepithelial cells in the early retina, and a mixture of neuroepithelial and Müller glia cells at later stages. Neuroepithelial and Müller glia cells have a similar, radial morphology and are summarily referred to herein as radial cells. DiI tracing of individual cells revealed that the radial cells span the entire width of the retina and terminated with end feet at the vitreal surface of the retina (Fig. 2b). Vimentin-staining (Fig. 2c) and

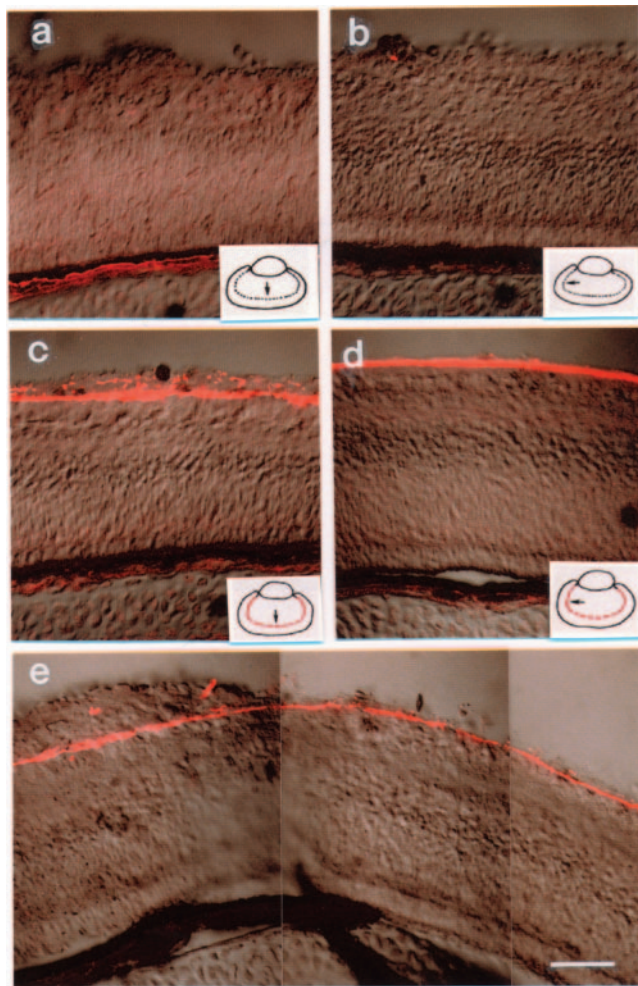


**FIGURE 1.** Cross sections through E10 retinas 5 days after injections of collagenase (a, b). Pulse-chase injections of collagenase followed by laminin-1/macroglobulin is shown in (c), (d), and (e). The retinas were stained for laminin-1. In eyes injected with collagenase, the central (a) and the newly developed peripheral retina (b) had no ILM. When the ILM was reconstituted with laminin-1, the central retina had an ectopic, regenerated ILM (c), and the newly generated retina has an ILM that is located at its normal site (d). The transition zone of displaced and normally located ILM is shown in (e). Bar, 50  $\mu$ m.

Dil tracing (Fig. 2d) showed that 5 days after ILM removal at E5, the vitreal processes were retracted by up to 150  $\mu$ m and terminated near the middle of the retina. As shown previously,<sup>18</sup> the retraction of radial cell processes occurs within hours after ILM disruption and is initially in the range of only 50  $\mu$ m. The 150- $\mu$ m retraction 5 days after ILM removal demonstrates that the radial cell processes continue to withdraw during further incubation.

When the ILM was disrupted at E7, the vitreal processes were distorted and grew growth cone-like terminals with multiple side branches (Fig. 2f), well different from the uniform end feet seen in age-matched control retinas (Fig. 2e). Yet, the processes were not retracted, as they all reached up to the vitreal surface of the retina (compare Fig. 2d with 2f). Thus, disruption of the ILM at E5 led to a retraction of radial cell end feet, whereas disruption of the ILM at E7 does not.

### Decline of GCs after ILM Removal

The first neurons in the retina are GCs. They are generated in a wave of differentiation that begins around E3 in the centro-

dorsal retina and ceases between E7 and E8 in the retinal periphery.<sup>27,28</sup> Up to E7, GCs were prominently but not exclusively located near the vitreal surface (Fig. 3b). By E8, they had established a well-defined cell layer (Fig. 3d). The number of GCs in control eyes increased to a maximum at E8 and then declined to a plateau at approximately E12 (Fig. 3i).

To investigate the fate of GCs after ILM removal, eyes were injected with collagenase at E5, and the location and number of retinal GCs was determined during the following 7 days of incubation. Twenty-four hours after removal of the ILM, GCs were more widely distributed than normal (Fig. 3a), and a defined GC layer never established during further incubation (Figs. 3c, 3e, 3f). During the first 2 days of survival, the number of GCs was approximately 25% higher than normal (Fig. 3i), confirming earlier studies.<sup>18</sup> From E8 onward, however, their number dramatically declined to <5% relative to the control

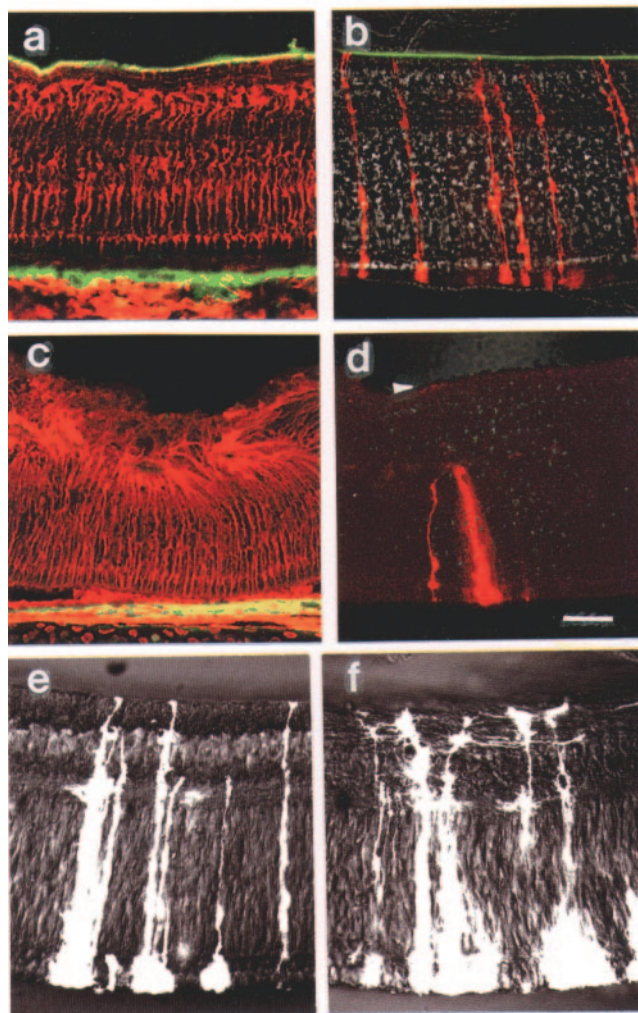


**FIGURE 2.** Cross sections through E10 control retinas (a, b) and E10 retinas from eyes injected with collagenase at E5 (c, d). The retinas were stained for laminin (green) and vimentin (a, c, red) or labeled with Dil (red) to reveal individual radial cells in the retina (b, d). In controls, the vitreal processes of the radial cells terminated at the ILM (a, b, green). In retinas whose ILM had been removed at E5, the radial cell processes terminated close to the middle of the retina, far short of the ILM (c, d). (d, arrowhead) The vitreal surface of the retina. When the ILM was disrupted at E7 (f) and the retinas labeled with Dil 5 days later at E12, the radial cells had not retracted (compare d with f). Rather, the vitreal processes grew side branches and displayed growth-cone-like terminals that differed from the regular array of end feet in E12 controls (e). Bar, 50  $\mu$ m.

(Figs. 3e, 3f, 3i). The few remaining GCs at E10 and E12 were randomly distributed in the central retina (Figs. 3e, 3f).

**GC Rescue after ILM Reassembly or Late ILM Disruption**

In eyes with a reconstituted ILM, GCs were more widely dispersed than normal, and many were ectopically positioned on the ILM (Figs. 3g, 5g).<sup>18</sup> During the first 2 days after the injections, the number of GCs was 25% higher than in control eyes (Fig. 3i).<sup>18</sup> Their number declined during further development, but leveled out by E10 to approximately 70% relative to the control (Figs. 3g, 3i), showing that ILM reconstitution rescued most of the GCs from cell death.

Collagenase was also injected into eyes of E7 embryos. Five days after removal of the ILM, the GC layer was less well organized than in the control eyes (Fig. 3h), but the number of GCs was in normal range (Fig. 3i). Thus, removal of the ILM at E7 did not lead to GC loss.

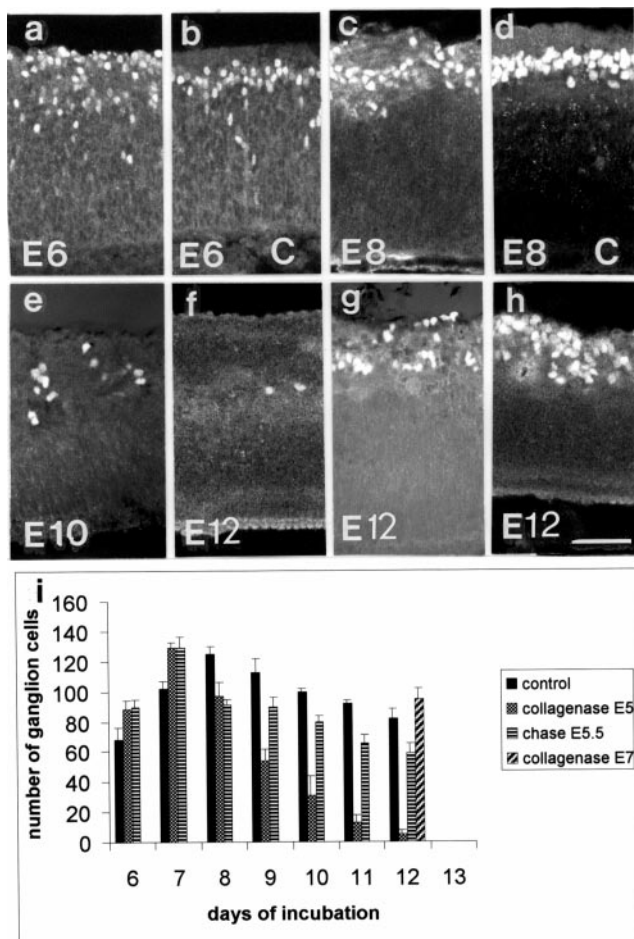


**FIGURE 3.** Cross sections through E6 (a), E8 (c), E10 (e), and E12 (f) retinas from eyes injected with collagenase at E5. Retinas from E6 and E8 control eyes (C) are shown for comparison in (b) and (d). The retinas were stained for islet 1 (a, b) and Brn3a (c-h) to visualize the nuclei of GCs. Note the dramatic decline and aberrant location of GCs at E10 and E12 (e, f), 5 and 7 days after ILM removal. (g) E12 retina in which the ILM was reconstituted 12 hours after its removal at E5; (h) an E12 retina in which the ILM was removed at E7. (i) The number of GCs in control and experimental retinas plotted against days in ovo. Experimental eyes were injected with collagenase at E5 (collagenase E5), E7 (collagenase E7), or pulse-chased with collagenase at E5 followed by laminin-1 at E5.5 (chase E5.5). Bar, 50  $\mu$ m.

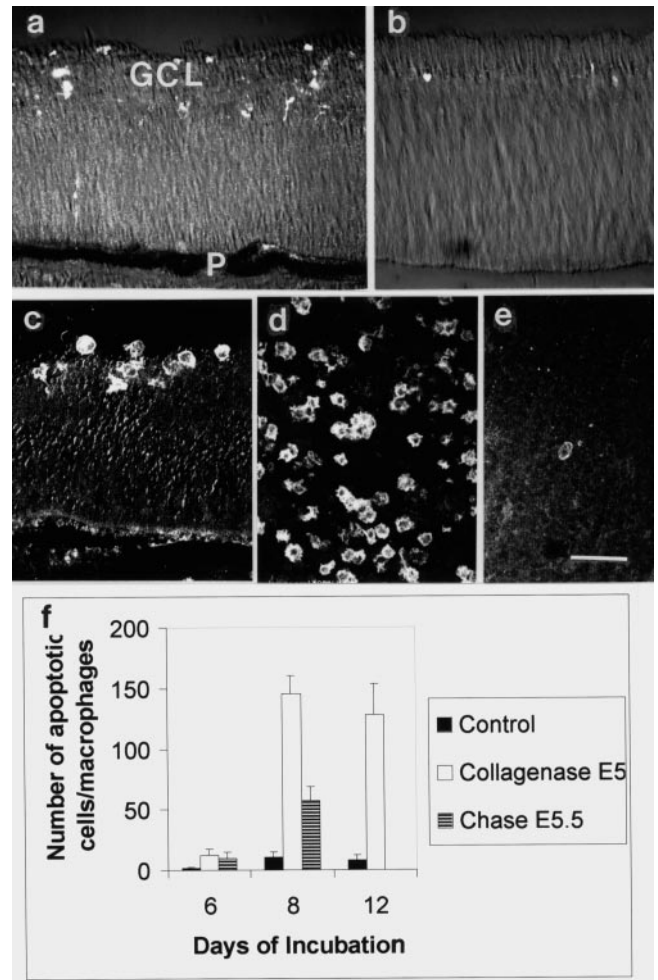


**FIGURE 4.** Cross sections and wholemounts of E10 chick retinas stained for cleaved caspase-3 (a, b) and CD44 (c-e). The disruption of the ILM at E5 resulted in a dramatic increase in apoptotic cells (a) and a major invasion of macrophages into the GC layer (GCL), as shown in cross sections (c) and wholemounts (d). Very few apoptotic cells and macrophages were detectable in the control retinas (b, e). P, pigment epithelium. (f) Number of apoptotic cells per cross section in E6 and E8 control eyes (Control), in eyes after ILM removal at E5 (Collagenase E5) and after ILM reconstitution at E5.5 (Chase E5.5). The number of macrophages in collagenase-treated eyes compared with control eyes is shown for E12 retinal wholemounts. Bar, 50  $\mu$ m.

**Effect of Early ILM Disruption on Apoptosis in GCs**

To find out whether GCs die by apoptosis or necrosis, we stained control and experimental retinas for cleaved caspase-3.<sup>29,30</sup> In normal control eyes, the number of positive cells per retinal cross section rose from 2 at E6 ( $n = 5$ ) to 11 at E8 ( $n = 4$ ; Figs. 4b, 4f). In experimental eyes, the number of apoptotic cells was >10 times higher (Figs. 4a, 4f), and almost all labeled cells were found in the GC layer (Fig. 4a). We also detected a major invasion of macrophages into the retinas of the experimental eyes (Figs. 4c, 4d), another hallmark of an ongoing apoptotic event.<sup>31</sup> The macrophages entered the eyes from the periorbital connective tissue around the ciliary body (not shown). The macrophages were detected within 24 hours of ILM disruption, and they were exclusively located in the ganglion cell and optic fiber layer (Fig. 4c). By counting in wholemounts, we found a 15-fold higher number of macrophages in experimental than in control retinas (compare Fig.

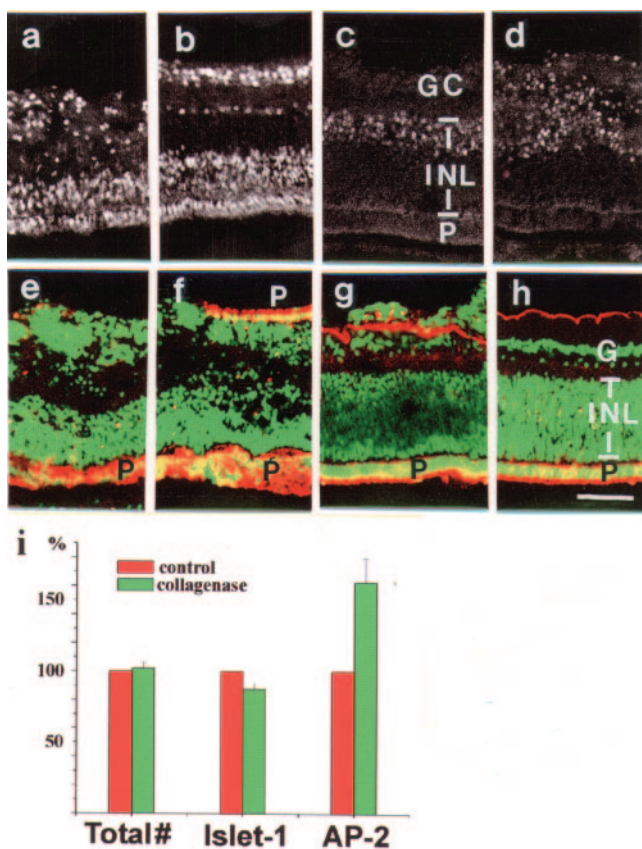


**FIGURE 5.** Cross sections through E12 retinas stained for islet-1 (a, b), AP-2 (c, d), and visinin plus laminin (e-h). Whereas the GC (GC) and amacrine cell layers are greatly disorganized after ILM removal at E5 (a), the inner nuclear (INL) and the photoreceptor layers (P) were less affected when compared with the control (b). Amacrine cells in control retinas were confined to a narrow band (c), whereas they are much more widely distributed in the experimental retinas (d) and much more numerous (i). The presence of a photoreceptor layer (P) in the experimental eyes was confirmed by staining for visinin (e). Segments in the peripheral retina of experimental eyes had an additional, ectopic photoreceptor layer (P) at the vitreal surface (f). The histology of retinas with a reconstituted ILM (g) was similar to that of a control retina (h). (e-h) Section stained for laminin to confirm the presence or absence of the ILM (red) and with a generic nuclear marker (green). (i) Comparison of the total number of retinal cells (Total #) and the number of Islet-1 and AP-2-positive neurons in control and collagenase-treated E12 eyes. The cell counts in experimental eyes are expressed as a percentage, using the cell count in control eyes as a 100% reference. Bar, 50  $\mu$ m.

4d with 4e and the 2 bars for E12 in 4f). In eyes with a reconstituted ILM, the number of apoptotic cells in E8 retinas was 5 times higher than in E8 controls, but 50% lower than in E8 retinas with no ILM at all (Fig. 4f).

We next determined whether ILM disruption leads to a disorganization of all retinal cell layers and causes random cell death. Three mAbs were used to label subsets of retinal neurons in E12 retinas, 7 days after ILM disruption: (1) an mAb to islet 1, which by E12 labeled the GCs, neurons of the lower part of the inner nuclear layer, a single layer of amacrine cells, and all photoreceptors (Fig. 5b), (2) an mAb to AP-2, a nuclear protein that is only expressed by amacrine cells (Fig. 5c), and an mAb to visinin to label photoreceptors (Fig. 5h). Results showed that most of the photoreceptors and Islet-1-positive neurons in the inner nuclear layer survived ILM disruption (compare Fig. 5a with 5b). The number of amacrine cells in experimental eyes was increased (compare Fig. 5c with 5d and

5i) and the AP-2-positive cells had expanded into the former GC layer (Fig. 5d). We hypothesize that the retina of a given developmental stage has a set number of cells and that the increase in amacrine cells in the experimental eyes occurs to compensate for the loss of GCs. Immunocytochemistry for visinin confirmed that the photoreceptor layer was not greatly altered after ILM disruption (compare Figs. 5e, 5h); however, we found segments in the peripheral retina in which an ectopic photoreceptor layer developed at the vitreal surface of the retina (Fig. 5f). To verify independently that ILM disruption did not lead to random cell death, we dissociated E12 experimental and control retinas into single-cell suspensions and determined the total cell number and the number of islet I-positive neurons. We found that the counts for total retinal cells in experimental and control retinas were similar (Fig. 5i). Twenty-six percent of the retinal cells were islet 1-positive neurons in control retinas, and a slightly reduced number was determined for the experimental retinas (Fig. 5i). The cell counts confirmed that ILM disruption does not lead to generic cell or neuron death in the retina.

Except for the ectopias in the GC layer, few histologic alterations were found in retinas with a reconstituted ILM (compare Fig. 5g with 5h as the control).

### GC Decline in Laminin- $\gamma$ 1 Mutant Mice

To confirm that GCs apoptosis is connected to ILM disruption and not the result of intraocular collagenase, we investigated the survival of GCs in mutant mice with a disrupted ILM. The mice carry a targeted deletion of the nidogen-binding module of the laminin  $\gamma$ 1 chain. BMs assemble in these mice, but they are fragile and rupture at random sites.<sup>14,23</sup> The mice die around birth from kidney agenesis and defects in lung development.<sup>23</sup> We examined the eyes of the mutants at E16.5 when most GCs have been generated. The eyes from homozygous mutant mice were distinguished from heterozygotes and control embryos by their slightly smaller size (compare Fig. 6b with 6c and 6d), by hemorrhages in either the anterior or the posterior eye chamber (Figs. 6a, 6c, 6d), and by genotyping. Hemorrhages were twice as common in the anterior as in the posterior eye chamber. High-power views of the homozygous-mutant retina showed multiple dysplasias at the vitreal surface with retinal cells penetrating into the vitreal body (Fig. 6f). Retinal ectopias were not connected to blood vessel rupture in the vitreal, since ectopias were also observed in eyes with blood vessel rupture in the anterior eye chamber. The ILM in the mutants had a normal ultrastructure, but was interrupted at multiple sites by cells penetrating the vitreal (Fig. 6h). In contrast, the retinal surface in the control was smooth (Fig. 6e), and the ILM was continuous (Fig. 6g).

As shown by staining for NCAM-180 and islet 1, the GC and optic fiber layers in mutant mice were located in their normal position near the vitreal surface of the retina (compare Fig. 7a with 7e and 7b with 7f), and backlabeling with DiI showed that the GCs sent out axons toward the optic disc (not shown). However, the GC layer in the mutant mice was thinner than in the control animals (compare Fig. 7a with 7e and 7b with 7f). Staining adjacent sections of mutant eyes for islet 1 (Fig. 7b) and laminin (Fig. 7c) revealed that some GCs formed ectopias on the retinal surface and that the ectopias coincided with gaps in the ILM. Further, the optic nerves of the mutant retinas (Fig. 7k) were  $51\% \pm 8\%$  ( $n = 3$ ) thinner than optic nerves in control mice (Fig. 7i). GC numbers were estimated by two methods: first, counting fluorescent cells in retinal whole-mounts after DiI backlabeling revealed that the number of GCs in retinas of mutant mice is reduced by 50% (Table 1). A similar 50% reduction of GCs was found by counting GCs in thin sections (Table 1). We also checked for alterations in radial cell

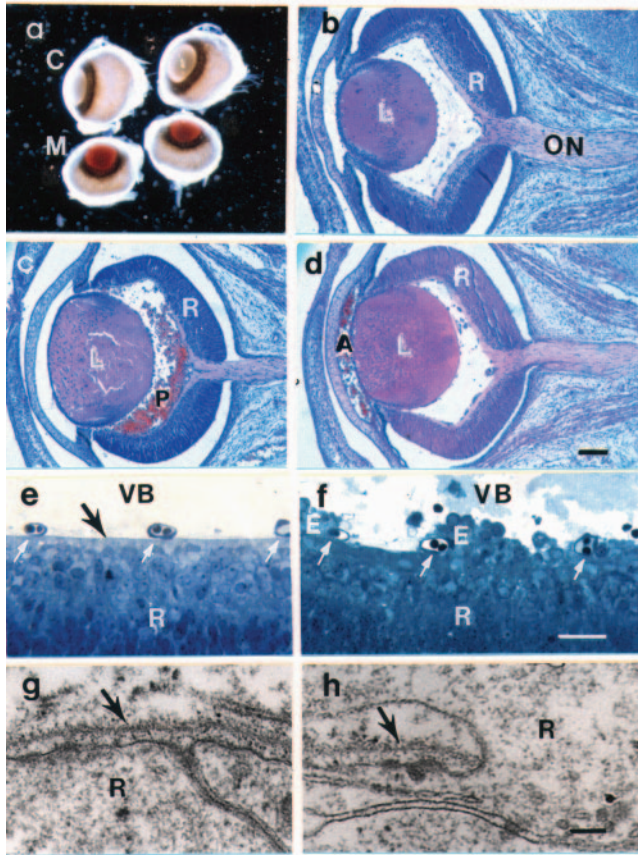


**FIGURE 6.** Eyes from E16.5 control and laminin-mutant mice. Mutant eyes (M) were distinguished from heterozygotic or wild-type control eyes (C) by their hemorrhages (a). The mutant eyes (M in a; sections in c, d) were slightly smaller than the control eyes (C in a; section in b), and cross sections showed that the hemorrhages were either in the posterior (P in c) or anterior eye chamber (A in d). L, lens; R, retina; ON, optic nerve. At high power, the control retinas (e) had a smooth vitreal surface (black arrow) with multiple hyaloid arteries (white arrows), whereas numerous ectopias (E) were seen along the vitreal surface of the mutant retinas (f). EM revealed a continuous, uninterrupted ILM (arrow) in the control retinas (g) and an interrupted ILM in the mutant mice (h). A retinal cell had breached the gap in the ILM (arrow) and entered the vitreous. Bar: (b, c, d) 100  $\mu$ m; (e, f) 50  $\mu$ m; (g, h) 50 nm.

morphology. Identical with chick, the mouse retinal neuroepithelium consisted of radially organized cells that terminated with an end foot at the vitreal surface (Fig. 7l). In mutant mice, we found, in addition to fully extended radial cells (Fig. 7m), a large number of cells that were retracted from the vitreal surface (Fig. 7n), similar to the retracted radial cells found in chick embryos with a disrupted ILM. GC death was not connected to blood vessel rupture in the vitreous, since GC decline was also observed in eyes with blood vessel ruptures in the anterior eye chamber.

Two observations showed that GCs in the mutant mice underwent apoptosis: we found approximately 10 times more cleaved caspase-3-labeled cells in mutant as in control retinas (compare Fig. 7d with 7h; Table 1). The caspase-positive cells were almost exclusively located in the GC layer (Fig. 7d). Second, in Nissl-stained retinal wholemounts we found 10 times more pyknotic nuclei in a given area of the GC layer in mutant mice as in the control. Third, macrophages were five times more abundant in the mutant retinas than in the control, and they were almost exclusively found in the GC layer (Table 1).

It is important to note that in embryonic mouse eyes all three laminin chains, nidogen-1, and collagen IV are synthesized by the lens and the ciliary body and not by GCs or retinal glia cells.<sup>32,33</sup> Further, the expression of BM proteins in the laminin-mutant mouse embryos is normal, and the ILM in the mutant mice includes all BM constituents of a normal ILM with the exception of nidogen, which is still synthesized, but no longer localizes to BMs due to the absence of its binding site in laminin- $\gamma$ 1.<sup>14,23</sup> By labeling the embryos with BrdU in utero,<sup>14</sup> we found that the rate of cell proliferation in the eyes of mutant and control mice was not visibly different (not shown), and that retinal ectopias were not due to aberrant proliferation rather the result of an abnormal cell migration, consistent with earlier observations in mouse cortex.<sup>14</sup>

**Neuron Survival In Vitro**

To find out whether ILM-dependent survival of GCs could also be demonstrated in vitro, chick retinal GCs were plated at low density on substrates of laminin-1, embryonic chick ILM with radial cells end feet, and plain ILMs without end feet. GCs were counted between 1 and 7 days after plating, and their identity as GCs was confirmed by staining for  $\beta$ -tubulin (Fig. 8), NCAM-180, neurofilament, and Islet-1 (not shown). The antibody stainings also demonstrated that GCs accounted for 70%  $\pm$  3.2%

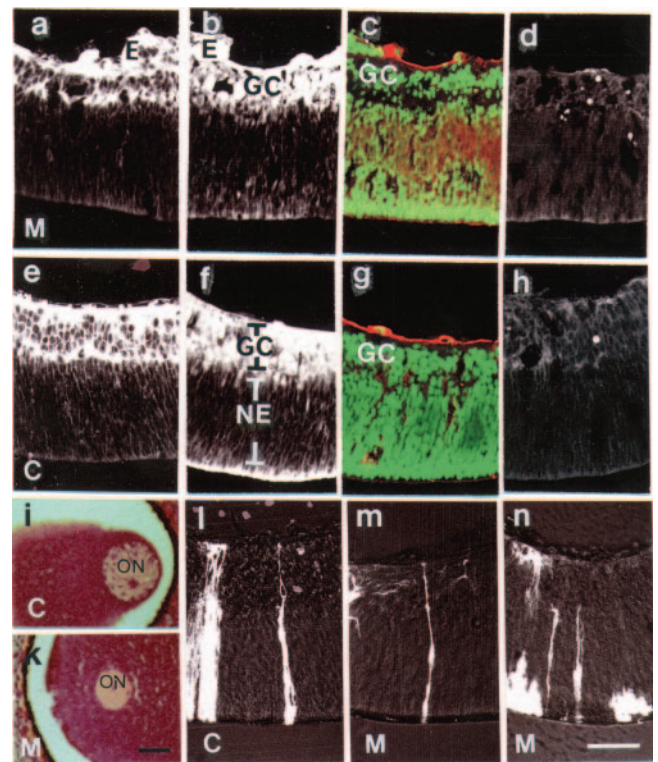


**FIGURE 7.** Cross sections through retinas from E16.5 mutant (a-d) and control mice (e-h). The sections were stained with antibodies to NCAM-180 (a, e), islet 1 (b, f), laminin (c, g), and activated caspase3 (d, h). Note the reduced size of the GC layer (GC; compare a with e; b with f) and the greater number of apoptotic cells (compare d with h) in the mutant compared with the control retinas. NE, neuroepithelial cell layer. Sections perpendicular through the optic nerves of a mutant (k) and a control embryo (i) shows the reduced diameter of the optic nerve (ON) in the mutant mice. Individual, DiI-labeled radial cells in control retinas extended long processes that reached the vitreal surface (l). In mutant mice, in addition to the normal radial cells with extension to the vitreal surface (m), a large number of cells had retracted processes that terminated short of the vitreal surface (n). Bar, 100  $\mu$ m.

TABLE 1. Counts of GCs, Apoptotic Cells and Macrophages in Mutant and Control Mice

	GC*	Apoptotic Cells†	Macrophages
Control	DiI: $39 \pm 2, n = 4$	Casp: $1.5 \pm 1, n = 4$	$4.3 \pm 2, n = 2$
Mutant	DiI: $20 \pm 3, n = 4$	Casp: $14 \pm n = 4$	$24 \pm 6, n = 2$
Control	Morph: $28 \pm 3, n = 4$	Nissl: $2 \pm 1, n = 2$	
Mutant	Morph: $14 \pm 2, n = 4$	Nissl: $36 \pm 5, n = 2$	

The counts are expressed as the means plus/minus SEM with *n* being the number of animals.

\* The number of GCs in mutant and control mice was determined in retinal wholemounts by backlabeling with DiI or in semithin sections according to morphologic criteria (Morph).

† Apoptotic cells were counted in cryostat sections after staining for activated caspase 3 (Casp) or in retinal wholemounts after Nissl staining (Nissl).

of the cells in the cultures. Further, BrdU labeling showed that cells did not proliferate in the serum-free cultures. Between 1 and 3 days in vitro, a similar number of GCs was counted on all three substrates (Figs. 8a, 8b, 8e). Likewise, there was extensive neurite outgrowth on all three substrates. From day 4 on, however, neurons on laminin-1 and plain ILM substrates (Fig. 8e) withdrew their processes and died, whereas they survived and maintained their processes on ILM with end feet (Figs. 8c, 8e). In addition, individual, well-differentiated neurons were found on the end feet monolayer substrates (Fig. 8c), whereas the few neurons that survived on laminin-1 and plain ILM substrates were always part of larger cell aggregates (Fig. 8d). Immunocytochemistry showed that dystroglycan (Fig. 8f) and integrin  $\beta 1$  (Fig. 8g) were abundantly present on the surface of the end feet, and both membrane proteins were detectable on the end feet throughout the entire 7-day culture period. When treated with detergent, integrin  $\beta 1$  and dystroglycan were no longer detectable (Fig. 8h). Further, cells migrating on the end feet monolayer dislodged the end feet leaving behind a track of plain ILM (Fig. 8f, arrow).<sup>34</sup> GCs within these cleared areas also underwent cell death within a 7-day incubation period, whereas adjacent GC cells on the end feet monolayer survived (not shown).

To account for potential extraction of substrate proteins by detergent or toxic effects of residual detergent, GCs were cultured on Triton X-100-treated laminin and untreated laminin. GCs counts and neurite outgrowth were identical on treated and nontreated laminin.

## DISCUSSION

### Requirements for ILM Assembly in the Retina

Our studies showed that when the ILM in embryonic chick eyes is disrupted, the eyes are unable to reconstitute a new ILM, even after a 7-day survival period. Further, in the absence of an ILM, the eyes were unable to assemble a new ILM in the newly developing, peripheral parts of the expanding retina, resulting in eyes with no ILM. ILM regeneration was initiated, however, by an intravitreal injection of laminin-1, and the presence of the reconstituted ILM allowed the assembly of a normally located ILM in the peripheral, newly generated retina. Based on our findings, we propose that the first step in the formation of an ILM is the binding of laminin-1 to cellular receptors such as dystroglycan<sup>35-37</sup> and integrin family members.<sup>38,39</sup> We assume that the binding of laminin-1 leads to the clustering of laminin receptors to radial cell end feet, facilitating the binding of additional laminin. The high densities allow adjacent laminin molecules to cross-link and bind other ILM constituents, such as agrin, perlecan, collagen XVIII, and nidogen, completing BM assembly. Consistent with our model, ILM disruption leads to the diffusion, and ILM reconstitution in a reclustering of dystroglycan to the neuroepithelial end feet plasma membrane.<sup>18</sup> Previous studies also showed that a 10-

20-fold higher than normal concentration of laminin-1 is necessary to induce the reclustering of laminin receptors to the neuroepithelial end feet,<sup>18</sup> which explains why the regeneration of the ILM does not occur spontaneously. Along the same line, we assume that the assembly of new ILM is facilitated by adjacent ILM through a preclustering of the laminin receptors to the neuroepithelial end feet. It is important to note that laminin-1 is not the only laminin member in the ILM and retina, as shown by previous studies in mouse and human,<sup>40</sup> yet it is laminin-1 that is able to reconstitute an entirely new ILM.

### ILM and GC Survival

Most of the GCs in chick embryos underwent apoptotic cell death when the ILM was removed at an early stage of eye development. The apoptosis of GCs was preventable by reconstituting the ILM, or by removing the ILM at a later stage of development, showing that collagenase by itself is nontoxic for GCs. The importance of the ILM in the survival of GCs was confirmed by the greatly reduced number of GCs in mutant mice with defective BMs.<sup>14,25</sup> The almost total loss of GCs in chick embryos after the complete removal of the ILM and the 50% reduction of GCs in the mutant mice with partial ILM disruption suggests a correlation in the degree of ILM disruption and the reduction in GCs. Evidence that GCs died by apoptosis came from the high number of caspase-3-positive cells in the GC layer and the massive invasion of macrophages, typical of inflammation-free apoptosis.<sup>31</sup>

Previous studies that lasted between 2 and 3 days showed that ILM removal leads to an increase in GCs in chick embryos.<sup>12,18</sup> Because the number of GCs is regulated by the Delta/Notch system,<sup>24,41</sup> we explained this increase by the greater dispersion of GCs after ILM disruption. The current results are consistent with the previous data by showing a 30% increase in GCs 48 hours after ILM removal. In the long run, however, GCs did not survive when the ILM was removed at an early stage of retinal development.

How does the absence of the ILM affect GC survival? A possible explanation may lie in the aberrant navigation of optic axons that follows ILM disruption.<sup>18</sup> It is conceivable that the misguided optic axons and their GCs are eliminated during the time of normal GC death.<sup>42</sup> The timing of GC death after ILM removal, however, argues against this notion: several studies have shown that maximum GC death in chick embryos after aberrant retinal axon navigation occurred between E12 and E14.<sup>43-45</sup> GC cell death after ILM disruption, however, peaked around E8, and was already complete by E11.

An alternative explanation for GC loss after ILM disruption may lie in the capacity of BMs to sequester growth factors. FGF, for example, binds to BMs and promotes neuron survival.<sup>28,46</sup> The ILM not only binds exogenous FGF,<sup>47</sup> but is also a site where endogenous FGF has been detected.<sup>48,49</sup> Several data, however, argue against ILM-bound growth factors' being responsible for GC survival: first, the removal of the ILM at E7

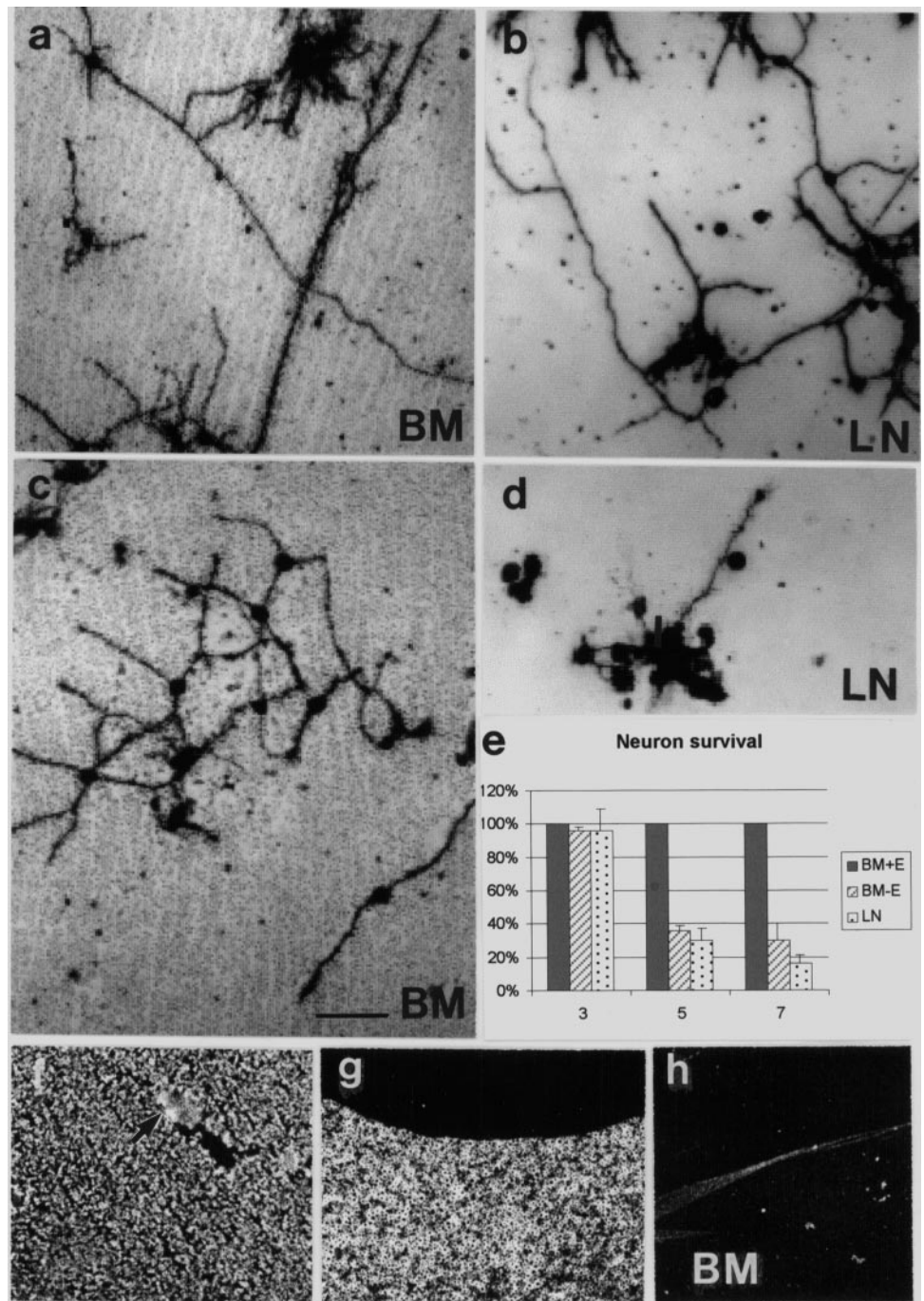


**FIGURE 8.** Retinal GCs cultured on ILM with neuroepithelial end feet (a, c) or on laminin-1 (b, d). The cells were cultured for 2 (a, b) or 5 (c–d) days. After 2 days in vitro, the neuron density on end feet (a) and laminin (b) substrates was similar, and the neurons generated long processes. After 5 days in vitro, many neurons had survived on the end feet monolayer (c), and they frequently existed as individual cells with long axonal and dendritic processes. On laminin, the few surviving neurons were always part of large cell aggregates (d) and had few, short processes. (e) Comparison of the number of surviving neurons on ILM with end feet (ILM+E), ILM without end feet (ILM–E), and laminin at 3, 5, and 7 days in culture. The presence of dystroglycan and integrin  $\beta 1$  in the end feet monolayer is shown in (f) and (g). A cell (f, arrow) had migrated for a short distance. In its wake, it left a trail in which the end feet had been dislodged from the underlying ILM. Dystroglycan and integrin (h) were no longer detectable after the end feet were removed with detergent. Bar, 100  $\mu\text{m}$ .

or later did not lead to a reduction in GCs, indicating that the ILM by itself or factors associated with it are not decisive for GC survival. Second, GCs did not survive when plated on plain ILM substrates, the site of bound growth factors.

Rather, our data argue in favor of a survival mechanism that requires the physical contact of GCs with the end feet of the radial cells: First, GCs survived best when grown in vitro on a monolayer of radial cell end feet. Second, GC cell death in vivo was always accompanied by the retraction of radial cell processes, and third, GCs were rescued by keeping radial cell retraction to a minimum. Further, GCs did not die when the ILM was removed at E7 or later, at a time when radial cells no longer need the ILM as an anchor to the vitreal retinal surface. Finally, the few remaining ganglion cells in basement mem-

brane-depleted retinas resided in the middle of the retina, next to the retracted radial cell end feet.

Our favorite hypothesis to explain the importance of the ILM for GC survival is that it anchors the radial cell end feet to the vitreal surface of the retina and thereby brings GCs and end feet in contact with each other. As shown previously and in this report, radial cell end feet retract, and their contact to the GCs is interrupted when the ILM is disrupted. As the connection to the radial cell end feet is lost, GCs die. It is well established that loss of substrate causes cells to undergo cell death, a process referred to as anoikis.<sup>50,51</sup> We speculate that the interaction of ganglion cells with the radial cells end feet confers a survival signal for GCs, possibly through an intracellular signaling cascade.<sup>52</sup>



Observations in other tissues and organs have shown that cell survival and the presence of BMs are linked: in preimplantation mutant mouse embryos, epiblast cells die when the endodermal BM is missing. The cells can be rescued by reconstituting the endodermal BM with exogenous laminin-1.<sup>53</sup> Similarly, notochordal cells in a mutant Zebrafish die due to the absence of the notochordal BM. The cells were rescued by laminin from wild-type tissue grafts.<sup>54</sup> In the mammary gland, cells that lose their BM do not differentiate and undergo apoptosis.<sup>55,56</sup> Finally, a recent study showed that degradation of laminin in the ILM is accompanied by GC death in mice after optic nerve ligation.<sup>57</sup> Thus, GC loss after ILM disruption is yet another instance in which cells die when the adjacent BM is destroyed and the cells have lost their natural substrate.

### Role of the ILM in Late Embryonic or Adult Retina

A surprising finding was that most GCs died when the ILM was removed at E5, but survived when the ILM was removed slightly later, at E7. By that time, the radial cells no longer need the ILM to extend their processes throughout the retina, providing further support for a correlation of GC survival and their contact to radial cell end feet. In the aged human eye, the removal of the ILM in macular hole surgery has no obvious detrimental effects, rather seems beneficial for the patient,<sup>58,59</sup> suggesting that the ILM has its main function during early embryogenesis and may be dispensable later.

### Acknowledgments

The authors thank Iris Janetti and Elke Burkhart for technical assistance.

### References

1. Timpl R. Macromolecular organization of basement membranes. *Curr Opin Cell Biol.* 1996;8:618-624.
2. Erickson AC, Couchman JR. Still more complexity in mammalian basement membranes. *J Histochem Cytochem.* 2000;48:1291-1306.
3. Colognato H, Winkelmann DA, Yurchenko P. Laminin polymerization induces a receptor-cytoskeleton network. *J Cell Biol.* 1999;145:619-631.
4. Timpl R, Wiedeman V, van Delden H., Furthmair H., Kuehn K. A network model of type IV collagen molecules in basement membranes. *Eur J Biochem.* 1981;120:203-211.
5. Yurchenko PD, Ruben GC. Basement membrane structure in situ: evidence for lateral association of the type IV collagen network. *J Cell Biol.* 1987;105:2559-2568.
6. Fox JM, Mayer U, Nischt R, Aumally M, Reinhardt D, Wiedemann H, et al. Recombinant nidogen consists of three globular domains and mediates binding of laminin to collagen IV. *EMBO J.* 1991;10:3137-3146.
7. Mayer U, Nischt R, Poeschl E, et al. A single EGF-like motif of laminin is responsible for high affinity nidogen binding. *EMBO J.* 1993;12:1879-1885.
8. Arikawa-Hirasawa E, Watanabe H, Takami H, Hassell JR, Yamada Y. Perlecan is essential for cartilage and cephalic development. *Nat Gen.* 1999;23:354-358.
9. Costell M, Gustafsson E, Aszodi A, et al. Perlecan maintains the integrity of cartilage and some basement membranes. *J Cell Biol.* 1999;147:1109-1122.
10. Gautam M, Noakes PG, Moscoso L, et al. Defective neuromuscular synaptogenesis in agrin-deficient mutant mice. *Cell.* 1996;85:525-535.
11. Fukui N, Eklund L, Marneros AG, et al. Lack of collagen XVIII/endostatin results in eye abnormalities. *EMBO J.* 2002;21:1535-1544.
12. Halfter W. Disruption of the retinal basal lamina during early embryonic development leads to a retraction of vitreal end feet, an increased number of ganglion cells, and aberrant axonal outgrowth. *J Comp Neurol.* 1998;397:89-104.
13. Halfter W, Schurer B. Disruption of the pial basal lamina during early avian embryonic development inhibits histogenesis and axonal pathfinding in the optic tectum. *J Comp Neurol.* 1998;397:105-117.
14. Halfter W, Dong S, Yip Y-P, Willem M, Mayer U. A critical function of the pial basement membrane in cortical histogenesis. *J Neurosci.* 2002;22:6029-6040.
15. Georges-Labouesse E. Essential role of  $\alpha 6$  integrins in cortical and retinal lamination. *Curr Biol.* 1998;8:983-986.
16. Graus-Porta D, Blaess S, Senften M, et al. Beta1-class integrins regulate the development of laminae and folia in the cerebral and cerebellar cortex. *Neuron.* 2001;16:367-379.
17. Moore SA, Saito F, Chen J, et al. Deletion of brain dystroglycan recapitulates aspects of congenital muscular dystrophy. *Nature.* 2002;418:422-425.
18. Halfter W, Dong S, Balasubramani M, Bier M. Temporary disruption of the retinal basal lamina and its effect on retinal histogenesis. *Dev Biol.* 2001;238:79-96.
19. Halfter W. A heparan sulfate proteoglycan in developing avian axonal tracts. *J Neurosci.* 1993;13:2863-2873.
20. Halfter W, Dong S, Schurer B, et al. Composition, synthesis, and assembly of the embryonic chick retinal basal lamina. *Dev Biol.* 2000;220:111-128.
21. Halfter W, Dong S, Schurer B, Cole GJ. Collagen XVIII is a basement membrane heparan sulfate proteoglycan. *J Biol Chem.* 1998;273:25404-25412.
22. Xiang M, Zhu L, Macke J, et al. The Brn-3 family of POU-domain factors: primary structure, binding specificity, and expression in subsets of retinal ganglion cells and somatosensory neurons. *J Neurosci.* 1995;15:4762-4785.
23. Willem M, Miosge N, Halfter W, et al. Specific ablation of the nidogen binding site in laminin gamma 1 interferes with kidney and lung development. *Development.* 2002;129:2711-2722.
24. Austin CP, Feldman DE, Ida JA, Cepko CL. Vertebrate retinal ganglion cells are selected from competent progenitors by the action of Notch. *Development.* 1995;121:3637-3650.
25. Halfter W, Reckhaus W, Kroger S. Nondirected axonal growth on basal lamina from avian embryonic neural retina. *J Neurosci.* 1987;7:3712-3722.
26. Bauch H, Stier H, Schlosshauer B. Axonal versus dendritic outgrowth is differentially affected by radial glia in discrete layers of the retina. *J Neurosci.* 1998;18:1774-1785.
27. Kahn A. Ganglion cell formation in the chick neural retina. *Brain Res.* 1973;63:285-290.
28. McCabe KL, Gunter EC, Reh TA. The development of the pattern of retinal ganglion cells in the chick retina: mechanisms that control differentiation. *Development.* 1999;126:5713-5724.
29. Srinivasan A, Roth KA, Sayers RD, et al. In situ immunodetection of activated caspase-3 in apoptotic neurons in the developing nervous system. *Cell Death Differ.* 1998;5:1004-1016.
30. DiCunto F, Imarisia S, Hirsch E, et al. Defective neurogenesis in citron kinase knockout mice by altered cytokinesis and massive apoptosis. *Neuron.* 2000;28:115-127.
31. Savill J, Fadok V. Corpse clearing defines the meaning of cell death. *Nature.* 2000;407:784-787.
32. Sarthy PV, Fu M. Localization of laminin B1 mRNA in retinal ganglion cells by in situ hybridization. *J Cell Biol.* 1990;110:2099-2108.
33. Dong L-J, Chung AE. The expression of the gene for entactin, laminin A, laminin B1 and laminin B2 in murine lens morphogenesis and eye development. *Differentiation.* 1991;48:157-172.
34. Halfter W, Diamantis I, Monard D. Migratory behavior of cells on embryonic retinal basal lamina. *Dev Biol.* 1988;130:159-275.
35. Blank M, Koulen P, Kroeger S. Subcellular concentration of  $\beta$ -dystroglycan in photoreceptors and glia cells of the chick retina. *J Comp Neurol.* 1997;389:668-678.
36. Henry MD, Campbell KP. A role of dystroglycan in basement membrane assembly. *Cell.* 1998;95:859-870.
37. Colognato H, Yurchenko P. Form and function: the laminin family of heterotrimers. *Dev Dynamics.* 2000;218:213-234.

38. Fleischmajer R, Utani A, MacDomald ED, et al. Initiation of skin basement membrane formation at the epidermo-dermal interface involves assembly of laminins through binding to cell membrane receptors. *J Cell Sci.* 1998;111:1929-1940.
39. Hering H, Koulen P, Kroger S. Distribution of integrin beta 1 subunit on radial glia cells in the embryonic and adult avian retina. *J Comp Neurol.* 2000;424:153-163.
40. Libby RT, Champliaud M-F, Claudepierre T, et al. Laminin expression in adult and developing retinae: evidence of two novel CNS laminins. *J Neurosci* 2000;20:6517-6528.
41. Dorsky RI, Chang WS, Rapaport DH, Harris WA. Regulation of neuronal diversity in the *Xenopus* retina by Delta signaling. *Nature.* 1997;385:67-70.
42. Rager G, Rager U. System-matching by degeneration, I: a quantitative electron microscopic study of the generation and degeneration of retinal ganglion cells in the chicken. *Exp Brain Res.* 1978;33:65-78.
43. Hughes WF, LaVelle A. The effect of early tectal lesions on development of in the retinal ganglion cell layer of chick embryos. *J Comp Neurol.* 1975;163:265-284.
44. Hughes WF, McLoon SC. Ganglion cell death during normal retinal development of the chick: comparison with cell death induced by early target field destruction. *Exp Neurol.* 1979;66:587-601.
45. Cook B, Portera-Cailliau C, Adler R. Developmental neuronal death is not a universal phenomenon among cell types in the chick embryonic retina. *J Comp Neurol.* 1998;396:12-19.
46. Walicke P, Cowan MW, Ueno N, Guillemin R. Fibroblast growth factor promotes survival of dissociated hippocampal neurons and enhances neurite extension. *Proc Natl Acad Sci USA.* 1986;83:3012-3016.
47. Fayein NA, Courtois Y, Jeanny JC. Ontogeny of basic fibroblast growth factor binding sites in mouse ocular tissues. *Exp Cell Res.* 1990;188:75-88.
48. Ohsato M, Hayashi H, Oshima K, Koji T, Nakane P. In situ localization of basic fibroblast growth factor protein and mRNA in the retina. *Ophthalmic Res.* 1997;29:24-30.
49. Chai L, Morris JE. Heparan sulfate in the inner limiting membrane of embryonic chicken retina binds basic fibroblast growth factor to promote axonal outgrowth. *Exp Cell Res.* 1999;160:175-185.
50. Frisch SM, Francis H. Disruption of epithelial cell-matrix interactions induces apoptosis. *J Cell Biol.* 1994;124:619-626.
51. Frisch SM, Vuori K, Ruoslahti E, Chan-Hui PY. Control of adhesion-dependent cell survival by focal adhesion kinase. *J Cell Biol.* 1996;134:793-799.
52. Chalasani S, Baribaud F, Coughlan CM, et al. The chemokine stromal cell-derived factor-1 promotes the survival of embryonic retinal ganglion cells. *J Neurosci* 2003;23:4601-4612.
53. Murray P, Edgar D. Regulation of programmed cell death by basement membranes in embryonic development. *J Cell Biol.* 2000;150:1215-1221.
54. Parson MJ, Pollard SM, Saude L, et al. Zebrafish mutants identify an essential role for laminins in notochord survival. *Development.* 2002;129:3137-3146.
55. Bodreau N, Werb Z, Bissell MJ. Suppression of apoptosis by basement membrane requires three-dimensional tissue organization and withdrawal from the cell cycle. *Proc Natl Acad Sci USA.* 1996;16:3509-3513.
56. Pullan S, Wilson J, Metcalf A, et al. Requirement of basement membrane for suppression of programmed cell death in mammary epithelium. *J Cell Sci.* 1996;109:631-642.
57. Chintala SK, Zhang X, Austin J, Fini ME. Deficiency in matrix metalloproteinase gelatinase B (MMP-9) protects against retinal ganglion cell death after optic nerve ligation. *J Biol Chem.* 2002;277:47461-47468.
58. Yoon HS, Brooks HL, Capone A, L'Hernault NL, Grossniklaus HE. Ultrastructural features of tissue removed during idiopathic macular hole surgery. *Am J Ophthalmol.* 1996;122:67-75.
59. Park DW, Sippley JO, Sneed SR, Dugel PU, Jacobsen JJ. Macular hole surgery with internal-limiting membrane peeling and intravitreal air. *Ophthalmology.* 1998;106:1392-1398.